

1 Article Type: Concepts & synthesis
2 Running title: Intrinsic predictability & forecasting

3

4 **Title: The intrinsic predictability of** 5 **ecological time series and its** 6 **potential to guide forecasting**

7

8 Frank Pennekamp^{1,§,*}, Alison C. Iles^{2,5,6,§}, Joshua Garland³, Georgina Brennan⁴, Ulrich
9 Brose^{5,6}, Ursula Gaedke⁷, Ute Jacob⁸, Pavel Kratina⁹, Blake Matthews¹⁰, Stephan Munch^{11, 12},
10 Mark Novak², Gian Marco Palamara^{1,13}, Björn C. Rall^{5,6}, Benjamin Rosenbaum^{5,6}, Andrea
11 Tabi¹, Colette Ward¹, Richard Williams¹⁴, Hao Ye¹⁵, Owen L. Petchey¹

12

13 § F. Pennekamp and A. Iles contributed equally to this work

14 * Corresponding author: frank.pennekamp@ieu.uzh.ch

15

16 ¹University of Zurich, Winterthurerstrasse 190, 8057, Zurich, Switzerland,

17 ²Oregon State University, 3029 Cordley Hall, Corvallis, OR 97331,

18 ³Santa Fe Institute, 1399 Hyde Park Rd, Santa Fe, NM 87501

19 ⁴Molecular Ecology and Fisheries Genetics Laboratory, School of Biological Sciences,

20 Bangor University, Bangor LL57 2UW, United Kingdom

21 ⁵EcoNetLab - Theory in Biodiversity Science, German Centre for Integrative Biodiversity

22 Research (iDiv) Halle-Jena-Leipzig, Deutscher Platz 5e, 04103, Leipzig, Germany

23 ⁶Institute of Biodiversity, Friedrich Schiller University Jena, Dornburger-Str. 159, 07743,

24 Jena, Germany

25 ⁷Institute for Biology, University of Potsdam
26 ⁸University of Hamburg
27 ⁹Queen Mary University of London
28 ¹⁰Eawag, Department of Aquatic Ecology, Center for Ecology, Evolution and
29 Biogeochemistry, Seestrasse 79, 6047, Kastanienbaum, Switzerland
30 ¹¹Fisheries Ecology Division, Southwest Fisheries Science Center, National Marine Fisheries
31 Service, National Oceanic and Atmospheric Administration, 110 Shaffer Rd., Santa Cruz, CA
32 95060, United States
33 ¹²Department of Ecology and Evolutionary Biology, University of California, Santa Cruz, CA
34 95064, United States
35 ¹³Eawag, Department Systems Analysis, Integrated Assessment and Modelling,
36 Überlandstrasse 133, 8600, Dübendorf, Switzerland
37 ¹⁴Slice Technologies, San Mateo
38 ¹⁵University of Florida, Wildlife Ecology and Conservation, 110 Newins-Ziegler Hall, PO
39 Box 110430, Gainesville, FL 32611-0430
40

41 Abstract

42 Successfully predicting the future states of systems that are complex, stochastic and
43 potentially chaotic is a major challenge. Model forecasting error (FE) is the usual measure of
44 success; however model predictions provide no insights into the potential for improvement.
45 In short, the *realized* predictability of a specific model is uninformative about whether the
46 system is inherently predictable or whether the chosen model is a poor match for the system
47 and our observations thereof. Ideally, model proficiency would be judged with respect to the
48 systems' *intrinsic* predictability – the highest achievable predictability given the degree to
49 which system dynamics are the result of deterministic v. stochastic processes. Intrinsic
50 predictability may be quantified with permutation entropy (PE), a model-free, information-
51 theoretic measure of the complexity of a time series. By means of simulations we show that a
52 correlation exists between estimated PE and FE and show how stochasticity, process error,
53 and chaotic dynamics affect the relationship. This relationship is verified for a dataset of 461
54 empirical ecological time series. We show how deviations from the expected PE-FE
55 relationship are related to covariates of data quality and the nonlinearity of ecological
56 dynamics. These results demonstrate a theoretically-grounded basis for a model-free
57 evaluation of a system's intrinsic predictability. Identifying the gap between the intrinsic and
58 realized predictability of time series will enable researchers to understand whether
59 forecasting proficiency is limited by the quality and quantity of their data or the ability of the
60 chosen forecasting model to explain the data. Intrinsic predictability also provides a model-
61 free baseline of forecasting proficiency against which modeling efforts can be evaluated.

62 **Key words:** time series analysis, Empirical Dynamic Modelling, permutation entropy,
63 information theory, population dynamics, forecasting

64 Introduction

65 Understanding and predicting the dynamics of complex systems are central goals for many
66 scientific disciplines (Weigend and Gershenfeld 1993, Hofman et al. 2017). Ecology is no
67 exception as environmental changes across the globe have led to repeated calls to make the
68 field a more predictive science (Clark et al. 2001, Petchey et al. 2015, Dietze 2017, Dietze et
69 al. 2018). One particular focus is *anticipatory predictions*, forecasting probable future states
70 in order to actively inform and guide decisions and policy (Mouquet et al. 2015, Maris et al.
71 2018). Robust anticipatory predictions require a quantitative framework to assess ecological
72 forecasting and diagnose when and why ecological forecasts succeed or fail.

73 Forecast performance is measured by **realized predictability** (see glossary), often
74 quantified as the correlation coefficient between observations and predictions, or its
75 complement, **forecasting error (FE)** measures, such as root mean squared error (RMSE).
76 Hence, realized predictability is in part determined by the model used as for any given
77 system, different models will give different levels of realized predictability. Furthermore, it
78 can be unclear, from realized predictability alone, whether the system is stochastic or the
79 model is a poor choice.

80 By contrast, the **intrinsic predictability** of a system is an absolute measure that
81 represents the highest achievable predictability (Lorenz 1995, Beekage et al. 2011). The
82 intrinsic predictability of a system can be approximated with model-free measure of time
83 series complexity, such as Lyapunov exponents or **permutation entropy** (Boffetta et al.
84 2002, Bandt and Pompe 2002, Garland et al. 2014). In principle, intrinsic predictability has
85 the potential to indicate whether the model, data, or system are limiting realized
86 predictability. Thus, if we know the intrinsic predictability of a system and its realized
87 predictability under specific models, the difference between the two is indicative of how
88 much predictability can be improved (Beekage et al. 2011).

89 Here we formalize a conceptual framework connecting intrinsic predictability and
90 realized predictability. Our framework enables comparative investigations into the intrinsic
91 predictability across systems and provides guidance on where and why forecasting is likely to
92 succeed or fail. We use simulations of the logistic map to demonstrate the behaviour of PE in
93 response to time series complexity and the effects of both process and measurement noise.
94 We confirm a general relationship between PE and FE, using a large dataset of empirical time
95 series and demonstrate how the quality, length, and **nonlinearity** in particular of these time
96 series influences the gap between intrinsic and realized predictability and the consequences
97 for forecasting.

98 **Conceptual framework**

99 The foundation for linking intrinsic and realized predictability lies in information theory and
100 builds on research demonstrating a relationship between PE and FE for complex computer
101 systems (Garland et al. 2014). Information theory was originally developed by Claude
102 Shannon as a mathematical description of communication (Shannon 1948) but has since been
103 applied across many disciplines. In ecology, several information-theoretic methods have
104 proved useful, including the Shannon biodiversity metric in which the probability of **symbol**
105 occurrences (see Box 1) is replaced by the probability of species occurrences (Jost 2006,
106 Sherwin et al. 2017), and the Akaike Information Criterion (Akaike 1974) which is widely
107 used for comparing the performance of alternative models (Burnham and Anderson 2002).
108 Given its importance to our framework, we first provide an introduction to information theory
109 with special attention to applications for ecological time series. Since our goal is to inform
110 where, when and why forecasting succeeds or fails; we then i) describe how **information**
111 may be partitioned into **new and redundant information** based on permutation entropy, ii)
112 demonstrate how redundant information is exploited by different forecasting models, and iii)

113 examine the relationship between permutation entropy and realized predictability and how it
114 can inform forecasting.

115 An information-theoretic perspective

116 A first step towards predicting the future of any system is understanding *if* the observations of
117 that system contain **information** about the future, i.e. does the system have a memory. The
118 total information in each observation can be thought of as a combination of information that
119 came from past states (i.e., **redundant information**) and information that is only available in
120 the present state (i.e., **new information**).

121 When there is a substantial amount of information transmitted from the past to the
122 present (figure 1Aiii), the system is said to be highly redundant. In other words, future states
123 depend greatly on the present and past states. In these cases, very little new information is
124 generated during each subsequent observation of the system and the resulting time series is,
125 in theory, highly predictable (has high intrinsic predictability).

126 Conversely, in systems dominated by stochasticity, the system state at each time point
127 is mostly independent of past states (figure 1Ai). Thus, all of the information will be “new”
128 information, and there will be little to no redundancy with which to train a forecasting model.
129 In this case, regardless of model choice, the system will not be predictable (has low intrinsic
130 predictability).

131 Imperfect observations introduce uncertainty or bias into time series, and thereby
132 affect the redundant information that is available or perceived. Observation errors in
133 particular will reduce the redundant information available to forecasting models, thus
134 lowering the realized predictability. We refer to this reduction as **lost information**, which is
135 not an innate property of the system but is the result of the practical limitations of making
136 measurements and any information-damaging processing of the data (figure 1B, Box 2). As
137 such, lost information can be mitigated and is an important leverage point for ecologists to

138 improve their forecasts. For example, replicate measurements or other forms of data
139 integration that increase estimation accuracy and reduce bias will reduce information loss and
140 can improve forecasts.

141 Permutation entropy

142 Permutation entropy (PE) is a measure of time series complexity that approximates the rate at
143 which new information is being generated along a time series (Box 1). PE approximates and
144 is inversely related to intrinsic predictability by quantifying how quickly the system generates
145 new information. Time series with low permutation entropy have high redundancy and are
146 expected to have high intrinsic predictability (Garland et al. 2014).

147 PE uses a symbolic analysis that translates a time series into a frequency distribution
148 of **words** (see glossary for definition). The frequency distribution of words is then used to
149 assess the predictability of the time series. For example, a time series in which a single word
150 (i.e. a specific pattern) dominates the dynamics has high redundancy and thus future states are
151 well predicted by past states. In contrast, a random time series, in which no single pattern
152 dominates, would produce a nearly uniform frequency distribution of words, with future
153 states occurring independently from past states. Hence, by quantifying the frequency
154 distribution of words, PE approximates how much information is transmitted from the past to
155 the present, corresponding to the intrinsic predictability of a time series.

156 When observations are imperfect PE measures the joint influence of new information
157 (from either internal or external processes) and lost information (due to the observation
158 process as well as data processing). We refer to the redundant information that is not lost and
159 remains available as **active information**, which is the information that can be exploited by
160 forecasting models.

161 Forecasting and redundant information

162 Realized predictability is highest when the chosen forecasting model exploits all the active
163 information contained in a time series. For illustration, we forecast the oscillating abundance
164 of a laboratory ciliate population (Veilleux 1976) with three different approaches (figure
165 1C): i) the mean of the time series (a model which uses relatively little of the active
166 information), ii) a linear autoregressive integrated moving-average model (ARIMA) that uses
167 the local-order structure of the time series in addition to the mean (a model which uses an
168 intermediate amount of the active information), and iii) empirical dynamic modelling (EDM)
169 that can incorporate **nonlinearities**, when present, in addition to the mean and local-order
170 structure (a model which can feasibly use more active information). The time series was split
171 into training data and test data. Forecasting models were fit to the training data and used to
172 make forward predictions among the test data. The forecast performance of the models (i.e.
173 the realized predictability) varied with the amount of information they used, which depended
174 on structural differences among the models that exploit the active information coming from
175 the past. EDM and ARIMA had similar performance suggesting that the time series entailed
176 little nonlinearities for the EDM to exploit.

177 The relationship between realized and intrinsic predictability

178 With a perfect forecasting model, realized predictability - measured by forecasting error (FE)
179 - and intrinsic predictability - measured by permutation entropy (PE) - will be positively
180 related. More specifically, the relationship will pass through the origin and monotonically
181 increase up to the maximum limit of $PE = 1$ (figure 1D, the boundary between the white and
182 grey regions; Garland et al. 2014). In the top right of this figure are systems with high PE
183 and therefore low redundancy and high forecasting error. In the bottom-left of the figure are
184 systems with low PE and therefore high redundancy and low forecast error. The boundary is
185 the limit for a perfect model that maximizes the use of active information.

186 Lost information complicates the interpretation of the PE - FE relationship by
187 obscuring the system's actual intrinsic predictability. We illustrate this case in figure 1D
188 using two hypothetical systems: one with high intrinsic predictability and a large amount of
189 lost information, and one with lower intrinsic predictability but relatively little lost
190 information. Despite the differences in the redundancy of two systems, the PE of their time
191 series can be very similar (even identical) because PE does not differentiate between new and
192 lost information.

193 For this example, both systems in figure 1D start with high FE relative to their PE.
194 Selecting more appropriate forecasting models causes a reduction in FE but no change in PE.
195 Reducing lost information (e.g. by increasing the frequency of measurements) decreases both
196 PE and FE. The system with a high redundancy and a low **Shannon entropy rate** has a
197 greater overall potential for improving forecasting skill through the recovery of lost
198 information. In contrast, the system with low redundancy has limited scope to further
199 improve forecasting skill; forecasting is less limited by lost information, but rather by its
200 lower redundancy. As such, the lowest possible forecast error will be substantially higher in
201 the second system than in the first system because the intrinsic predictability of the second is
202 inherently lower and cannot be changed.

203 **Materials & Methods**

204 **Forecasting with EDM**

205 Empirical dynamic modelling is a set of nonlinear forecasting techniques brought to the
206 attention of ecologists through the work of Sugihara (1994). The method is based on the idea
207 that a system's attractor generating the dynamics of a time series can be reconstructed via
208 delay coordinate embedding (Takens 1981, Sauer et al. 1991), which can then be used to
209 forecast system dynamics (Lorenz 1969, Farmer and Sidorowich 1987, Sauer et al. 1991,

210 Casdagli and Eubank 1992, Smith 1992, Weigend and Gershenfeld 1993, Garland and
211 Bradley 2011, 2015, Garland et al. 2014). These methods are rooted in a deterministic
212 dynamic system's paradigm and hence require at least some determinism in the temporal
213 course of the system and hence are unsuitable for purely stochastic systems. However, they
214 have proven to reliably forecast ecological systems even in the presence of process and
215 measurement noise typical for ecological systems (Sugihara & May 1990, Ye et al. 2015) and
216 are constantly improved to deal with issues such as observation error and nonstationarity of
217 ecological systems (Munch et al. 2017). The variant of these methods we use in this
218 manuscript is based on the simplex projection and S-map method (Sugihara 1994) through
219 the rEDM package (<https://ha0ye.github.io/rEDM/>).

220 The EDM approach first identifies the optimal embedding dimension E of the training
221 data by fitting a model using simplex projection (Sugihara 1994). The embedding dimension
222 E determines the number of temporal lags used for the delay coordinate embedding. We
223 tested values for E between 1 and 10 and selected the value of E with the highest forecast
224 skill using leave-one-out cross validation (Sugihara 1994). We then fitted the tuning
225 parameter θ on the training data using the S-map model. θ describes the nonlinearity of the
226 system and was varied in 19 steps (0, 0.0001, 0.0003, 0.001, 0.003, 0.01, 0.03, 0.1, 0.3, 0.5,
227 0.75, 1.0, 1.5, 2, 3, 4, 6, 8, and 10) to find the lowest error using leave-one-out cross
228 validation on the training data.

229 In contrast to other forecasting methods such as ARIMA, the EDM approach searches across
230 multiple time series models by finding the optimal in-sample combination of embedding
231 dimension and tuning parameter using cross-validation. Due to this model selection step,
232 EDM tests a suite of forecasting models equal to the number of combinations of θ and E .
233 When θ is 0, the EDM model corresponds to an autoregressive model of the order of the

234 embedding dimension (i.e. an AR3 model if $E = 3$). Values of θ greater than 0 can account
235 for increasing degrees of state-dependence.

236 Assessment of forecast error

237 We quantified forecasting error with the root mean squared error (Hyndman and Koehler
238 2006),

239

$$240 \quad \text{RMSE} = \sqrt{\frac{\sum_{i=1}^k (c_i - p_i)^2}{k}},$$

241

242 where k is the number of observed c_i values (i.e. abundances) and p_i are their corresponding
243 predicted values. To compare forecast errors across time series that vary widely in units and
244 variability, we normalized their RMSE by the range of observed values using

245

$$246 \quad \text{nRMSE} = \frac{\text{RMSE}}{\max(c_i) - \min(c_i)}.$$

247

248 Smaller nRMSE corresponds to smaller forecasting error.

249 Calculation of permutation entropy

250 We calculated the weighted permutation entropy (WPE) of time series using the methods
251 outlined in Box 1.

252 Logistic Map Time Series

253 To demonstrate how both intrinsic and realized predictability change along a continuum from
254 simple to complex and chaotic time series, we applied permutation entropy to time series
255 from a well known population dynamic model, the Logistic Map:

$$256 \quad x_{t+1} = r x_t (1 - x_t).$$

257 This model maps the current year's population size to next year's population size with simple
258 density-dependence between non-overlapping generations. Although simple, this first-order,
259 nonlinear function produces a wide range of dynamical behavior, from stable and oscillatory
260 equilibria to chaotic dynamics (May and others 1976). We include this range of behavior by
261 simulating the logistic map for 500 incremental growth rates between $r = 3.4$ and $r = 3.9$. We
262 simulated each growth rate for 10,000 time steps keeping the last 3000 times steps for
263 analysis. Weighted permutation entropy of time series was calculated for permutation order,
264 m , from 3 to 5 and for time delay, τ , from 1 to 4. For simplicity, we will refer to weighted
265 permutation entropy only in the results section and use the generic term permutation entropy
266 everywhere else. Forecasting error for each time series was calculated using the normalized
267 root mean squared error of an EDM forecast of the last 200 time steps.

268 Because ecological systems are influenced by both deterministic and stochastic
269 drivers and the logistic map is purely deterministic, we sought to evaluate how stochasticity
270 (noise) affects weighted permutation entropy and forecast error. To do so, we independently
271 added both observational noise and process noise to the simulated population sizes by
272 drawing random values from Gaussian distributions with standard deviations of either 0,
273 0.0001, 0.001, or 0.01 (Bandt and Pompe 2002). We also investigated the effect of non-
274 Gaussian noise distributions on WPE and FE, although in this case we applied it to the Ricker
275 model which does not have an upper bound of 1 like the logistic map (see appendix S1 for
276 details). If the new population size was not between 0 and 1, a new value was drawn.
277 Observational noise was added to the population size time series after the simulation, whereas
278 process noise was added to population size at each time step during the simulation.

279 Empirical Time Series Data

280 For empirical evidence of a relationship between permutation entropy and forecasting error,
281 we examined a large variety of ecological time series that differ widely in complexity and

282 data quality. We further investigated whether deviations from the expected general
283 relationship can be explained by time series covariates such as measurement error (proxied
284 here by whether the data originated from field versus lab studies), the nonlinearity of the time
285 series (as quantified by the theta parameter of an EDM), or time series length. This allowed
286 us to identify possible predictors of time series complexity and the potential with which the
287 time series of a system can be moved along the permutation-forecasting error (PE-FE)
288 relationship to maximize realized predictability.

289 Time series databases and processing

290 We compiled laboratory time series from the literature and field time series from the publicly
291 available Global Population Dynamic Database (GPDD) for our analysis. The GPDD is the
292 largest compilation of univariate time series available, spanning a wide range of geographic
293 locations, biotopes and taxa (NERC Centre for Population Biology, 1999, Inchausti & Halley
294 2001). The GDPP database was accessed via the rGDPP package in R
295 (<https://github.com/ropensci/rgpdd>). We added laboratory time series from studies by Becks
296 et al. (2005), Fussmann et al. (2000), and the datasets used in a meta-analysis by Hiltunen et
297 al. (2014). Time series with less than 30 observations, gaps greater than 1 time step and more
298 than 15% of values being equal (and hence having the same rank in the ordinal analysis, i.e.
299 ties) were excluded, resulting in a total of 461 time series. Each time series was divided into
300 training (initial $\frac{2}{3}$ of the time series) and test data (the last $\frac{1}{3}$ of the time series), with the
301 EDM model performing best on the training set being used to estimate forecast error in the
302 test set. We calculated the weighted permutation entropy (WPE) of each empirical time series
303 using a permutation order, m , of 3 and a time delay, τ , of 1. Results were robust to the choice
304 of $m \in [2, 5]$ and $\tau \in [1, 4]$. The three different ways to deal with ties (i.e. “random”, “first”,
305 “average”) did not qualitatively affect the results, with results being robust to variation in
306 time series minimum length and tie percentage

307 Statistical analysis

308 All analyses were performed in the statistical computing environment R (R Development
309 Core Team 2016). We used the lme4 package to fit mixed models to investigate the
310 relationship between forecast error and permutation entropy (Bates et al. 2015), with
311 forecasting error being the dependent variable. We included the data source (i.e. publication)
312 as a random grouping variable to account for possible non-independence across time series
313 from the same study. The independent variables were permutation entropy, the data type, the
314 number of observations (N), the proportion of zeros in the time series (zero_prop), the
315 proportion of ties in the time series (ties_prop), and, from the EDM analysis, the nonlinearity
316 (θ) and the embedding dimension (E) of the time series. The data type, i.e. whether time
317 series were measured in the lab or in the field, was included with our hypothesis being that
318 lab measurements have lower observation error. Zero and tie proportions were included as
319 they pose problems to the estimation of PE, as do short time series (see Box 2). Three of our
320 predictor variables, namely PE, θ and E are potentially measured with error violating an
321 assumption of linear models (Quinn and Keough 2002). However, alternative approaches
322 such as reduced major axis regression are only advised if the relationship between response
323 and predictors is symmetric (Smith 2009). We therefore did not adjust for error, but note that
324 the strength of the relationship of our predictors may be potentially underestimated due to
325 measurement error in the predictors (Quinn and Keough 2002). Model diagnostics showed
326 normally and homogeneously distributed residuals. Code to reproduce the analysis can be
327 found on Github: XXX.

328 Results

329 Logistic Map Time Series

330 The expected relationship between weighted permutation entropy and forecasting error
331 occurred in the simulations of the logistic map. Both WPE and FE generally increase as the
332 growth rate, r , increases and the dynamics of the logistic map enter the realm of deterministic
333 chaos (figure 4D). Correspondingly, both WPE and FE decline when chaotic dynamics
334 converge to limit cycles (figure 4, gold example with $r \approx 3.84$).

335 The effect of stochastic noise on the WPE-FE relationship depended on the type of
336 noise considered. While process noise strongly affects both WPE and FE (figure 5A)
337 observational noise affects forecasting error more strongly than WPE (figure 5B). Indeed, the
338 relationship between WPE and FE is largely obscured at high process noise but remains
339 positive at high observational noise (figure 5A, B, top panels), particularly when dynamics
340 are chaotic. When the dynamics are chaotic, the weighting in WPE is very effective at
341 reducing the influence of observational noise on estimates of permutation entropy. However,
342 when the dynamics exhibit stable limit cycles, WPE is sensitive to noise and this depends
343 strongly on the chosen time delay, τ , and word length, m . This effect is a statistical artefact
344 caused by tied ranks in the words that are then influenced by noise. For instance, applying
345 $\tau=2$ for a 2-point limit cycle with a small amount of noise produces a WPE close to one,
346 appearing as white noise as all permutations occur with equal probability. Limit cycles are
347 best analyzed with $\tau=1$ to capture the oscillations, although with $m=3$ small amounts of noise
348 still result in two permutations occurring with equal frequency (1-3-2 or 2-3-1) and so WPE
349 is elevated with respect to the no-noise case despite the high redundancy of the limit cycles
350 (figure 5B, dark blue and gold points; see appendix S2: Fig. S1 for details). The effect of
351 stochasticity on the WPE-FE relationship is generally robust to the chosen model and noise

352 distribution (see appendix S1: Fig. S1, S2 for the analysis of the Ricker model with
353 multiplicative lognormal noise).

354 Empirical Time Series Results

355 The 461 empirical time series vary in length (median = 50, min = 30, max = 197) and, as
356 measured by WPE, complexity (median = 0.84, min = 0.076, max = 1). Forecasting error
357 (nRMSE) ranges from 0.0000093 to 1.37, with a median of 0.19. Our analysis shows the
358 expected positive relationship between permutation entropy and forecast error, with more
359 complex time series (high WPE) yielding higher forecasting error (Table 1, center panel of
360 figure 6). No difference in mean forecast error nor a difference in slope is detected between
361 time series originating from lab or field studies (Table 1). Exploring the effects of time series
362 covariates indicates that longer time series had lower FE, whereas time series with larger
363 dimensionality (E) and greater nonlinearity (θ) as measured by EDM show higher FE (Table
364 1). These covariates increase the amount of variation in FE explained across time series to
365 35% (CI: 29 - 42%). An analysis of the partial R^2 of all fixed effects in the model revealed
366 that PE individually explained the largest amount of variation among predictors (21%, CI: 15
367 - 27%), followed by time series length (18%, CI: 12 - 24%), time series nonlinearity θ (6%,
368 CI: 2 - 10%) and the chosen embedding dimension E (4%, 1 - 9%). Zero and tie proportions,
369 as well as whether time series were from the field or the lab (type) explained less than 1% of
370 the observed variation.

371 The PE v. FE relationship allows us to identify time series which were predicted
372 better, equal to or worse than expected regarding their complexity (figure 6 a-f). Time series
373 'b' and 'c' fall along the expected relationship and hence are well predicted despite large
374 differences in complexity. Time series 'a' shows a clear trend which is well predicted. In
375 contrast, time series 'd'-'f' have higher than expected forecast error. Time series 'd' shows
376 higher than expected error due to a strong outlier in the predicted values early in the test

377 dataset. Time series ‘e’ is consistently poorly predicted, potentially due to wrong model
378 choice or due to the short time series length. Time series ‘f’ is complex (high PE) with
379 predictions missing the ongoing downward trend in the test data.

380 Discussion

381 The urgent need for ecologists to provide operational forecasts to managers and decision
382 makers requires that we understand when and why forecasts succeed or fail (Clark et al.
383 2001, Petchey et al. 2015, Dietze 2017). We propose that the measurement of the intrinsic
384 predictability of an ecological system can help reveal the origin of predictive uncertainty and
385 indicate whether and how it can be reduced.

386 Our results show that realized and intrinsic predictability positively covary. The
387 simulation study revealed that the relationship can be obscured by stochastic process noise,
388 while measurement noise led to more scatter but preserved the positive slope (figure 5).
389 Although process noise often dominates over measurement noise in ecological time series
390 (Ahrestani et al. 2013), the positive relationship between intrinsic and realized predictability
391 we revealed across a wide range of empirical time series supports the applicability of our
392 framework. In our analysis, permutation entropy explained the largest amount of variation
393 (21%) in forecast error, followed by time series length, dimensionality and nonlinearity,
394 jointly accounting for 35% of the variation. Time series that fell onto the expected
395 relationship (figure 6b,c) were well predicted given their complexity, whereas clear outliers
396 (e.g. figure 6e) would not require the use of PE to be identified as such. The relationship
397 however allowed us to identify potential problems with forecasts of time series that have
398 reasonable forecasts error, but which may be affected by overfitting (figure 6a), outliers
399 (figure 6d) or regime shifts (figure 6e) that may have gone unnoticed when looking at FE

400 alone, particularly if applying automated or semi-automated forecasting methods across
401 hundreds or thousands of time series (White et al. 2018).

402 **The value of intrinsic predictability to guide forecasting**

403 A major advantage of permutation entropy is the independence from any assumed underlying
404 model of the system, which makes this “model-free” method highly complementary to
405 existing model-based approaches. For instance, Dietze (2017) recently proposed a model-
406 based framework that partitions the contribution of various factors to predictive uncertainty,
407 including the influence of initial conditions, internal dynamics, external forcing, parameter
408 uncertainty and process error at different scales. If, for example, the dominant factor affecting
409 near-term forecasts is deemed to be internal dynamics, then insight into intrinsic
410 predictability would demonstrate how stable those internal dynamics are. Similarly, if a lot of
411 variation remains unexplained by the model (i.e. the process error not explained by the
412 known internal dynamics, initial conditions, external drivers, and estimated parameters), then
413 “model-free” methods can provide insight into whether that variation is largely stochastic or
414 contains unexploited structure that could be captured with further research into the driving
415 deterministic processes. Finally, permutation entropy could be applied to the predicted
416 dynamics of models to ascertain whether they accurately reflect properties of the observed
417 dynamics, such as their complexity, similar to comparing the nonlinearity of a time series
418 with the dynamics of the best model using the EDM framework (Storch et al. 2017). Thus,
419 intrinsic predictability provides diagnostic insights into predictive uncertainty and guidance
420 for improving predictions.

421 **Comparative assessments of intrinsic predictability**

422 The model-free nature of permutation entropy is advantageous in cross-system and cross-
423 scale comparative studies of predictability. Whereas comparing all available forecasting

424 methods on a given time series and predicting with the best-performing method would give
425 us the best realized predictability (e.g., Ward et al. 2014), we would miss out on the
426 comparative insight gained from aligning very different time series along the complexity
427 gradient quantified by permutation entropy. Such a comparison could afford insight into
428 whether intrinsic predictability differs across levels of ecological organization, taxonomic
429 groups, habitats, geographic regions or anthropogenic impacts (Petchey et al. 2015).
430 Determining the most appropriate covariates of monitored species (e.g. body size, life history
431 traits, and trophic position) that minimize lost information would also inform monitoring
432 methods. Furthermore, monitoring how realized and intrinsic predictability converge over
433 time provides a means to judge improvements in predictive proficiency (Petchey et al. 2015,
434 Houlahan 2016, Dietze 2017). To do so, we need to apply available forecasting models to the
435 same time series and measure their forecast error in combination with their intrinsic
436 predictability. The monitoring of predictive proficiency has greatly advanced weather
437 forecasting as a predictive science (Bauer et al. 2015). The analysis of univariate time series
438 presented here only begins to put the intrinsic predictability of different systems into
439 perspective. A primary goal is hence to expand the availability of long-term, highly resolved
440 time series to determine potential covariates and improve our general understanding of
441 ecological predictability (Ward et al. 2014, Petchey et al. 2015).

442 **Reliable assessment of intrinsic predictability**

443 Permutation entropy requires time series data of suitable length and sampling frequency to
444 infer the correct permutation order and time delay (Riedl et al. 2013). Given the complexity
445 of many ecological time series, the method rarely works with less than 30 data points (see
446 recommendations in box 1). We acknowledge these as fairly stringent requirements for
447 ecological time series. Time series measured at the appropriate time scales over long periods
448 of time are rare, despite the knowledge that they are among the most effective approaches at

449 resolving long-standing questions regarding environmental drivers (Lindenmayer et al. 2012,
450 Hughes et al. 2017, Giron-Nava et al. 2017). This problem is beginning to be resolved with
451 automated measurements of system states, such as chlorophyll-a concentrations in aquatic
452 systems (Blauw et al. 2018, Thomas et al. 2018), assessment of community dynamics in
453 microbiology (Trosvik et al. 2008, Faust et al. 2015, Martin-Platero et al. 2018), and
454 phenological (Pau Stephanie et al. 2011) and flux measurements (Dietze 2017). Such high-
455 frequency, long-term data are likely to provide a more accurate picture of the range of
456 possible system states, even when systems are non-ergodic and change through time (e.g.
457 figure 6f). In fact, given the ease with which it is computed, PE can be assessed with a
458 moving window across time or space to determine if a system is stationary or changing. As
459 such, PE may be used as an early warning signal for system tipping points and critical
460 transitions (Scheffer et al. 2009, Dakos and Soler-Toscano 2017) or to evaluate the effect of a
461 management intervention on the system state.

462 Currently, there is no generally accepted approach to calculate uncertainty in PE
463 values and compare whether two PE values are statistically different. Approaches such as
464 comparing empirical estimates of PE to white-noise time series or parametric bootstrapping
465 have been suggested (Little and Kane 2016, Traversaro and O. Redelico 2018), however,
466 these approaches are not free from challenges and may provide an overconfident picture of
467 uncertainty. One suggestion is for the practitioner to rely on persistence over parameter
468 space. That is, slightly modify the parameters of the calculation (change m and τ) and see if
469 the results change. If the results do not change, this should suggest a higher degree of
470 reliability. Nevertheless, this limitation does not diminish the usefulness of PE for regression-
471 based applications such as those presented and we are confident that increased usage of PE
472 will result in methodological advances such as uncertainty estimation.

473 Although the full potential of permutation entropy to guide forecasting is not yet
474 realized, many other fields are starting to take advantage of its diagnostic potential. In
475 paleoclimate science, permutation entropy has proven useful for detecting hidden data
476 problems caused by outdated laboratory equipment (Garland et al. 2016, 2018), and in the
477 environmental sciences it has provided insight into model-data deviations of gross primary
478 productivity to further understand the global carbon cycle (Sippel et al. 2016). In
479 epidemiology a recent study on the information-theoretic limits to forecasting of infectious
480 diseases concluded that for most diseases the forecast horizon is often well beyond the time
481 scale of outbreaks, implying prediction is likely to succeed (Scarpino and Petri 2017).
482 Our result showing that permutation entropy covaries with forecast error highlights the
483 potential of using permutation entropy to better understand time series predictability in
484 ecology and other disciplines.

485 **Acknowledgements**

486 This paper originates from the “sPRED - Synthesizing Predictability Research of Ecological
487 Dynamics” working group, supported by the Synthesis Centre of the German Centre for
488 Integrative Biodiversity Research (DFG-FZT-118). FP, AT and OP benefitted from funding
489 by the Swiss National Science Foundation (grant 31003A_159498 to OP). AI was supported
490 by the Alexander von Humboldt Foundation. JG was supported by an Omidyar Fellowship
491 from the Santa Fe Institute. HY is supported by the Gordon and Betty Moore Foundation’s
492 Data-Driven Discovery Initiative through grant GBMF4563 to Ethan P. White. BR, BCR and
493 UB acknowledge support by the German Research Foundation (FZT 118). We thank Gregor
494 Fussmann and Lutz Becks for generously sharing time series data from microcosm
495 experiments.

496

497 References

- 498 Ahrestani, F. S., M. Hebblewhite, and E. Post. 2013. The importance of observation versus
499 process error in analyses of global ungulate populations. *Scientific Reports* 3:3125.
- 500 Akaike, H. 1974. A new look at the statistical model identification. *IEEE Transactions on*
501 *Automatic Control* 19:716–723.
- 502 Amigó, J. M., M. B. Kennel, and L. Kocarev. 2005. The permutation entropy rate equals the
503 metric entropy rate for ergodic information sources and ergodic dynamical systems.
504 *Physica D: Nonlinear Phenomena* 210:77–95.
- 505 Bandt, C. 2005. Ordinal time series analysis. *Ecological Modelling* 182:229–238.
- 506 Bandt, C., and B. Pompe. 2002. Permutation Entropy: A Natural Complexity Measure for
507 Time Series. *Physical Review Letters* 88:174102.
- 508 Bates, D., M. Mächler, B. Bolker, and S. Walker. 2015. Fitting Linear Mixed-Effects Models
509 Using lme4. *Journal of Statistical Software* 67:1–48.
- 510 Bauer, P., A. Thorpe, and G. Brunet. 2015. The quiet revolution of numerical weather
511 prediction. *Nature* 525:47–55.
- 512 Beckage, B., L. J. Gross, and S. Kauffman. 2011. The limits to prediction in ecological
513 systems. *Ecosphere* 2:art125.
- 514 Becks, L., F. M. Hilker, H. Malchow, K. Jürgens, and H. Arndt. 2005. Experimental
515 demonstration of chaos in a microbial food web. *Nature* 435:1226–1229.
- 516 Blauw, A. N., E. Benincà, R. W. P. M. Laane, N. Greenwood, and J. Huisman. 2018.
517 Predictability and environmental drivers of chlorophyll fluctuations vary across
518 different time scales and regions of the North Sea. *Progress in Oceanography* 161:1–
519 18.
- 520 Boffetta, G., M. Cencini, M. Falcioni, and A. Vulpiani. 2002. Predictability: a way to
521 characterize complexity. *Physics Reports* 356:367–474.
- 522 Burnham, K. P., and D. R. Anderson. 2002. *Model Selection and Multi-Model Inference: A*
523 *Practical Information-Theoretic Approach*. Springer, New York.

- 524 Casdagli, M., and S. Eubank, editors. 1992. *Nonlinear Modeling and Forecasting*. 1 edition.
525 CRC Press, Redwood City, Calif.
- 526 Clark, J. S., S. R. Carpenter, M. Barber, S. Collins, A. Dobson, J. A. Foley, D. M. Lodge, M.
527 Pascual, R. P. Jr, W. Pizer, C. Pringle, W. V. Reid, K. A. Rose, O. Sala, W. H.
528 Schlesinger, D. H. Wall, and D. Wear. 2001. *Ecological Forecasts: An Emerging*
529 *Imperative*. *Science* 293:657–660.
- 530 Dakos, V., and F. Soler-Toscano. 2017. Measuring complexity to infer changes in the
531 dynamics of ecological systems under stress. *Ecological Complexity* 32:144–155.
- 532 Dietze, M. C. 2017. Prediction in ecology: a first-principles framework. *Ecological*
533 *Applications* 27:2048–2060.
- 534 Dietze, M. C., A. Fox, L. M. Beck-Johnson, J. L. Betancourt, M. B. Hooten, C. S. Jarnevich,
535 T. H. Keitt, M. A. Kenney, C. M. Laney, L. G. Larsen, H. W. Loescher, C. K. Lunch, B.
536 C. Pijanowski, J. T. Randerson, E. K. Read, A. T. Tredennick, R. Vargas, K. C.
537 Weathers, and E. P. White. 2018. Iterative near-term ecological forecasting: Needs,
538 opportunities, and challenges. *Proceedings of the National Academy of*
539 *Sciences*:201710231.
- 540 Fadlallah, B., B. Chen, A. Keil, and J. Príncipe. 2013. Weighted-permutation entropy: A
541 complexity measure for time series incorporating amplitude information. *Physical*
542 *Review E* 87:022911.
- 543 Farmer, J. D., and J. J. Sidorowich. 1987. Predicting chaotic time series. *Physical Review*
544 *Letters* 59:845–848.
- 545 Faust, K., L. Lahti, D. Gonze, W. M. de Vos, and J. Raes. 2015. Metagenomics meets time
546 series analysis: unraveling microbial community dynamics. *Current Opinion in*
547 *Microbiology* 25:56–66.
- 548 Fussmann, G. F., S. P. Ellner, K. W. Shertzer, and N. G. Hairston. 2000. Crossing the hopf
549 bifurcation in a live predator-prey system. *Science (New York, N.Y.)* 290:1358–1360.

550 Garland, J., and E. Bradley. 2011. Predicting Computer Performance Dynamics. Pages 173–
551 184 in J. Gama, E. Bradley, and J. Hollmén, editors. *Advances in Intelligent Data*
552 *Analysis X*. Springer Berlin Heidelberg.

553 Garland, J., and E. Bradley. 2015. Prediction in projection. *Chaos: An Interdisciplinary*
554 *Journal of Nonlinear Science* 25:123108.

555 Garland, J., R. James, and E. Bradley. 2014. Model-free quantification of time-series
556 predictability. *Physical Review E* 90:052910.

557 Garland, J., T. R. Jones, E. Bradley, R. G. James, and J. W. C. White. 2016. A First Step
558 Toward Quantifying the Climate’s Information Production over the Last 68,000 Years.
559 Pages 343–355 *Advances in Intelligent Data Analysis XV*. Springer, Cham.

560 Garland, J., T. R. Jones, E. Bradley, M. Neuder, and J. W. C. White. 2018. Climate entropy
561 production recorded in a deep Antarctic ice core. arXiv:1806.10936 [physics].

562 Giron-Nava, A., C. James, A. Johnson, D. Dannecker, B. Kolody, A. Lee, M. Nagarkar, G.
563 Pao, H. Ye, D. Johns, and G. Sugihara. 2017. Quantitative argument for long-term
564 ecological monitoring. *Marine Ecology Progress Series* 572:269–274.

565 Hiltunen, T., N. G. Hairston, G. Hooker, L. E. Jones, and S. P. Ellner. 2014. A newly
566 discovered role of evolution in previously published consumer–resource dynamics.
567 *Ecology letters* 17:915–923.

568 Hofman, J. M., A. Sharma, and D. J. Watts. 2017. Prediction and explanation in social
569 systems. *Science* 355:486–488.

570 Houlahan, J. E. 2016. The priority of prediction in ecological understanding. *Oikos*.

571 Hughes, B. B., R. Beas-Luna, A. K. Barner, K. Brewitt, D. R. Brumbaugh, E. B. Cerny-
572 Chipman, S. L. Close, K. E. Coblenz, D. Nesnera, K. L. S. T. Drobnitch, J. D.
573 Figurski, B. Focht, M. Friedman, J. Freiwald, K. K. Heady, W. N. Heady, A. Hettinger,
574 A. Johnson, K. A. Karr, B. Mahoney, M. M. Moritsch, A.-M. K. Osterback, J. Reimer,
575 J. Robinson, T. Rohrer, J. M. Rose, M. Sabal, L. M. Segui, C. Shen, J. Sullivan, R.
576 Zuercher, P. T. Raimondi, B. A. Menge, K. Grorud-Colvert, M. Novak, and M. H.

577 Carr. 2017. Long-Term Studies Contribute Disproportionately to Ecology and Policy.
578 *BioScience* 67:271–281.

579 Hyndman, R. J., and A. B. Koehler. 2006. Another look at measures of forecast accuracy.
580 *International Journal of Forecasting* 22:679–688.

581 Jost, L. 2006. Entropy and diversity. *Oikos* 113:363–375.

582 Lindenmayer, D. B., G. E. Likens, A. Andersen, D. Bowman, C. M. Bull, E. Burns, C. R.
583 Dickman, A. A. Hoffmann, D. A. Keith, M. J. Liddell, A. J. Lowe, D. J. Metcalfe, S. R.
584 Phinn, J. Russell-Smith, N. Thurgate, and G. M. Wardle. 2012. Value of long-term
585 ecological studies. *Austral Ecology* 37:745–757.

586 Little, D. J., and D. M. Kane. 2016. Permutation entropy of finite-length white-noise time
587 series. *Physical Review E* 94:022118.

588 Lorenz, E. N. 1969. Atmospheric Predictability as Revealed by Naturally Occurring
589 Analogues. *Journal of the Atmospheric Sciences* 26:636–646.

590 Lorenz, E. N. 1995. Predictability: a problem partly solved.

591 Maris, V., P. Huneman, A. Coreau, S. Kéfi, R. Pradel, and V. Devictor. 2018. Prediction in
592 ecology: promises, obstacles and clarifications. *Oikos* 127:171–183.

593 Martin-Platero, A. M., B. Cleary, K. Kauffman, S. P. Preheim, D. J. McGillicuddy, E. J. Alm,
594 and M. F. Polz. 2018. High resolution time series reveals cohesive but short-lived
595 communities in coastal plankton. *Nature Communications* 9:266.

596 May, R. M., and others. 1976. Simple mathematical models with very complicated dynamics.
597 *Nature* 261:459–467.

598 Mouquet, N., Y. Lagadeuc, V. Devictor, L. Doyen, A. Duputié, D. Eveillard, D. Faure, E.
599 Garnier, O. Gimenez, P. Huneman, F. Jabot, P. Jarne, D. Joly, R. Julliard, S. Kéfi, G.
600 J. Kergoat, S. Lavorel, L. Le Gall, L. Meslin, S. Morand, X. Morin, H. Morlon, G.
601 Pinay, R. Pradel, F. M. Schurr, W. Thuiller, and M. Loreau. 2015. Predictive ecology
602 in a changing world. *Journal of Applied Ecology* 52:1293–1310.

603 Munch, S. B., V. Poynor, and J. L. Arriaza. 2017. Circumventing structural uncertainty: A
604 Bayesian perspective on nonlinear forecasting for ecology. *Ecological Complexity*
605 32:134–143.

606 Pau Stephanie, Wolkovich Elizabeth M., Cook Benjamin I., Davies T. Jonathan, Kraft Nathan
607 J. B., Bolmgren Kjell, Betancourt Julio L., and Cleland Elsa E. 2011. Predicting
608 phenology by integrating ecology, evolution and climate science. *Global Change*
609 *Biology* 17:3633–3643.

610 Petchey, O. L., M. Pontarp, T. M. Massie, S. Kéfi, A. Ozgul, M. Weilenmann, G. M.
611 Palamara, F. Altermatt, B. Matthews, J. M. Levine, D. Z. Childs, B. J. McGill, M. E.
612 Schaepman, B. Schmid, P. Spaak, A. P. Beckerman, F. Pennekamp, and I. S.
613 Pearse. 2015. The ecological forecast horizon, and examples of its uses and
614 determinants. *Ecology Letters* 18:597–611.

615 Quinn, G. G. P., and M. J. Keough. 2002. *Experimental design and data analysis for*
616 *biologists*. Cambridge University Press.

617 R Core Team. 2018. *R: A language and environment for statistical computing*. R Foundation
618 for Statistical Computing, Vienna, Austria.

619 Riedl, M., A. Müller, and N. Wessel. 2013. Practical considerations of permutation entropy.
620 *The European Physical Journal Special Topics* 222:249–262.

621 Sauer, T., J. A. Yorke, and M. Casdagli. 1991. Embedology. *Journal of Statistical Physics*
622 65:579–616.

623 Scarpino, S. V., and G. Petri. 2017. On the predictability of infectious disease outbreaks.
624 arXiv:1703.07317 [physics, q-bio].

625 Scheffer, M., J. Bascompte, W. A. Brock, V. Brovkin, S. R. Carpenter, V. Dakos, H. Held, E.
626 H. van Nes, M. Rietkerk, and G. Sugihara. 2009. Early-warning signals for critical
627 transitions. *Nature* 461:53–59.

628 Shannon, C. E. 1948. A mathematical theory of communication. *The Bell System Technical*
629 *Journal* 27:379–423.

630 Sherwin, W. B., A. Chao, L. Jost, and P. E. Smouse. 2017. Information Theory Broadens the
631 Spectrum of Molecular Ecology and Evolution. *Trends in Ecology & Evolution* 0.

632 Sippel, S., H. Lange, M. D. Mahecha, M. Hauhs, P. Bodesheim, T. Kaminski, F. Gans, and
633 O. A. Rosso. 2016. Diagnosing the Dynamics of Observed and Simulated Ecosystem
634 Gross Primary Productivity with Time Causal Information Theory Quantifiers. *PLOS*
635 *ONE* 11:e0164960.

636 Smith, L. A. 1992. Identification and prediction of low dimensional dynamics. *Physica D:*
637 *Nonlinear Phenomena* 58:50–76.

638 Smith, R. J. 2009. Use and misuse of the reduced major axis for line-fitting. *American*
639 *Journal of Physical Anthropology* 140:476–486.

640 Storch, L. S., S. M. Glaser, H. Ye, and A. A. Rosenberg. 2017. Stock assessment and end-
641 to-end ecosystem models alter dynamics of fisheries data. *PLOS ONE* 12:e0171644.

642 Sugihara, G. 1994. Nonlinear Forecasting for the Classification of Natural Time Series.
643 *Philosophical Transactions: Physical Sciences and Engineering* 348:477–495.

644 Takens, F. 1981. Detecting strange attractors in turbulence. Pages 366–381 *Dynamical*
645 *Systems and Turbulence, Warwick 1980*. Springer, Berlin, Heidelberg.

646 Thomas, M. K., S. Fontana, M. Reyes, M. Kehoe, F. Pomati, and T. Coulson. 2018. The
647 predictability of a lake phytoplankton community, over time-scales of hours to years.
648 *Ecology Letters* 21:619–628.

649 Traversaro, F., and F. O. Redelico. 2018. Confidence intervals and hypothesis testing for the
650 Permutation Entropy with an application to epilepsy. *Communications in Nonlinear*
651 *Science and Numerical Simulation* 57:388–401.

652 Trosvik, P., K. Rudi, T. Næs, A. Kohler, K.-S. Chan, K. S. Jakobsen, and N. C. Stenseth.
653 2008. Characterizing mixed microbial population dynamics using time-series
654 analysis. *The ISME Journal* 2:707–715.

655 Veilleux, B. 1976. The analysis of a predatory interaction between *Didinium* and
656 *Paramecium*. Master's Thesis, University of Alberta, Canada.

657 Ward, E. J., E. E. Holmes, J. T. Thorson, and B. Collen. 2014. Complexity is costly: a meta-
658 analysis of parametric and non-parametric methods for short-term population
659 forecasting. *Oikos* 123:652–661.

660 Weigend, A. S., and N. A. Gershenfeld. 1993. *Time Series Prediction: Forecasting The*
661 *Future And Understanding The Past*. 1 edition. Routledge, Reading, MA.

662 White, E. P., G. M. Yenni, S. D. Taylor, E. M. Christensen, E. K. Bledsoe, J. L. Simonis, and
663 S. M. Ernest. 2018. Developing an automated iterative near-term forecasting system
664 for an ecological study. *bioRxiv*:268623.

665

666 **Glossary**

667 **Active information:** The amount of information that is available to forecasting models

668 (redundant information minus lost information; figure 1).

669 **Forecasting error (FE):** A measure of the discrepancy between a model's forecasts and the

670 observed dynamics of a system. Common measures of forecast error are root mean squared

671 error and mean absolute error.

672 **Entropy:** Measures the average amount of information in the outcome of a stochastic

673 process.

674 **Information:** Any entity that provides answers and resolves uncertainty about a process.

675 When information is calculated using logarithms to the base two (i.e. information in bits), it is

676 the minimum number of yes/no questions required, on average, to determine the identity of

677 the symbol (Jost 2006). The information in an observation consists of information inherited

678 from the past (redundant information), and of new information.

679 **Intrinsic predictability:** the maximum achievable predictability of a system (Beckage et al.

680 2011).

681 **Lost information:** The part of the redundant information lost due to measurement or

682 sampling error, or transformations of the data (figure 1).

683 **New information, Shannon entropy rate:** The Shannon entropy rate quantifies the average

684 amount of information per observation in a time series that is unrelated to the past, i.e., the

685 new information (figure 1).

686 **Nonlinearity:** When the deterministic processes governing system dynamics depend on the

687 state of the system.

688 **Permutation entropy (PE):** permutation entropy is a measure of the complexity of a time

689 series (Bandt and Pompe 2002) that is negatively correlated with a system's predictability

690 (Garland et al. 2014). Permutation entropy quantifies the combined new and lost information.

691 PE is scaled to range between a minimum of 0 and a maximum of 1.

692 **Realized predictability:** the achieved predictability of a system from a given forecasting
693 model.

694 **Redundant information:** The information inherited from the past, and thus the maximum
695 amount of information available for use in forecasting (figure 1).

696 **Symbols, words, permutations:** symbols are simply the smallest unit in a formal language
697 such as the letters in the English alphabet i.e., {"A", "B", ..., "Z"}. In information theory the
698 alphabet is more abstract, such as elements in the set {"up", "down"} or {"1", "2", "3"}.

699 Words, of length m refer to concatenations of the symbols (e.g., up-down-down) in a set.

700 Permutations are the possible orderings of symbols in a set. In this manuscript, the words are
701 the permutations that arise from the numerical ordering of m data points in a time series.

702 **Weighted permutation entropy (WPE):** a modification of permutation entropy (Fadlallah et
703 al. 2013) that distinguishes between small-scale, noise-driven variation and large-scale,
704 system-driven variation by considering the magnitudes of changes in addition to the rank-
705 order patterns of PE.

706

707 **Boxes**

708 **Box 1 Theory and estimation of PE and WPE**

709 Information theory provides several measures for approximating how much new information
710 is expected per observation of a system (e.g. the Shannon-entropy rate and the Kolmogorov-
711 Sinai entropy). However, these measures are only well defined for infinite sequences of
712 discrete random variables and can be quite challenging to approximate for continuous random
713 variables, especially if one only has a finite set of imperfect observations. Permutation
714 entropy is a measure aimed at robustly approximating the Shannon-entropy rate of a times
715 series (or the Kolmogorov-Sinai entropy if the time series is stationary).

716 Rather than estimating probability mass functions from **symbol** frequencies or
717 frequencies of sequences of symbols, as is done with traditional estimates of the Shannon-
718 entropy rate, permutation entropy uses the frequencies of orderings of sequences of values; it
719 is an ordinal analysis (see figure 2 for a visual explanation). The ordinal analysis of a time
720 series maps the successive time-ordered elements of a time series to their value-ordered
721 permutation of the same size. As an example, if $[x_1, x_2, x_3] = [11, 6, 8]$ then its ordinal pattern,
722 or word, $\phi([x_1, x_2, x_3])$, is 2-3-1 since $x_2 \leq x_3 \leq x_1$ (see red time series fragment in figure 2A).
723 PE is calculated by counting the frequencies of these words (or **permutations**) that arise after
724 the time series undergoes this ordinal analysis. That is, given a time series (figure 2A), let
725 S_m be defined as the set of all permutations (possible words) π of order (word length) m and
726 time delay τ , describing the delay between successive points in the time series (figure 2B for
727 $m = 3$ and $\tau = 1$). For each permutation $\pi \in S_m$ we estimate its relative frequency of
728 occurrence for the observed time series after performing ordinal analysis on each delay
729 vector, $p(\pi) = \frac{|\{i \mid i \leq N - m, \phi([x_i, x_{i+\tau}, \dots, x_{i+m\tau}]) = \pi\}|}{N - m + 1}$, where $|\cdot|$ denotes set cardinality (figure 2C). Then
730 permutation entropy of order $m \geq 2$ is calculated as $h(m) = -\sum_{\pi \in S_m} p(\pi) \log_2(p(\pi))$.

731 Since, $0 \leq h(m) \leq \log_2(m!)$, it is common to normalize permutation entropy by dividing by
 732 $\log_2(m!)$. With this convention, maximal $h(m) = 1$ and minimal $h(m)$ is equal to 0. Since in
 733 the infinite word length limit, permutation entropy is equivalent to the Kolmogorov-Sinai
 734 entropy as long as the observational uncertainty is sufficiently small (Amigó et al. 2005), we
 735 can approximate the intrinsic predictability of an ecological time series by computing $1 -$
 736 $h(m)$.

737 For the ordinal analysis of a time series, ranks are only well defined if all values are
 738 different. If some values are equal (so called 'ties'), the ordinal analysis is not possible.
 739 Several approaches are available to break the ties: the "first" method results in a permutation
 740 with increasing values at each index set of ties, and analogously "last" with decreasing
 741 values. The "random" method puts these in random order whereas the "average" method
 742 replaces them by their mean, and "max" and "min" replaces them by their maximum and
 743 minimum respectively, the latter being the typical sports ranking.

744 In contrast, an ordinal analyses is also affected by small scale fluctuations due to
 745 measurement noise which can obscure the influence of large scale system dynamics.

746 **Weighted permutation entropy (WPE)** reduces the influence of small-scale fluctuations by
 747 taking into account the relative magnitudes of the time series values within each word
 748 (Fadlallah et al. 2013). That is, each word's $(X_t = [x_t, x_{t-\tau}, \dots, x_{t-\tau(m-1)}])$ contribution to
 749 the probability mass function is weighted by its variance, viz., $w(X_t) \equiv var(X_t)$. Using this
 750 weighting function, the weighted probability of each permutation is estimated by: $p_w(\pi) =$
 751 $\sum_{t \leq N-m} w(X_t) \cdot \delta$ where $\delta(x, y) = 1$ if and only if $x = y$ and $\delta(x, y) = 0$ otherwise. The
 752 weighted permutation entropy of order $m \geq 2$ is then defined as $h_w(m) =$
 753 $-\sum_{\pi \in S_m} p_w(\pi) \log_2(p_w(\pi))$. Similar to PE, the weighted permutation entropy is normalized
 754 by $\log_2(m!)$. We use weighted permutation entropy for all analyses presented in this
 755 manuscript.

756 The estimation of PE to time series requires specifying a order m and time delay τ .
757 The shorter the chosen word length, the fewer possible words there are and the better we can
758 estimate permutation frequencies. However, the ability to distinguish patterns is limited by
759 the possible number of unique permutations. Hence, when word lengths are too short or too
760 long, the frequency distribution is more uniform. In practice the total length of the time series
761 limits the choice of possible word lengths and hence the number of unique words that can be
762 resolved (Riedl et al. 2013). Regarding the time delay τ , most applications to study the
763 complexity of a time series use a $\tau = 1$ (Riedl et al. 2013). If $\tau > 1$, Bandt (2005) notes the
764 interesting property of the permutation entropy to be small, if the series has main period p for
765 $\tau = p / 2$ and $3 p / 2$, and to be large for $\tau = p$ and $\tau = 2 p$. We refer to Riedl et al. (2013) who
766 provide practical considerations regarding setting permutation order m and time delay τ .

767

768 **Box 2 with information on the limitations of PE / WPE**

769 When analyzing time series, ecologists typically employ a number of data pre-processing
770 methods. These methods are used to reduce low-frequency trends or periodic signals
771 (detrending), reduce high-frequency variation (smoothing), standardize across the time series
772 or reduce the influence of extreme values (transformation), deal with uncertain or missing
773 data points (gap or sequence removal, and interpolation), to examine specific time step sizes
774 (downsampling), or to combine different time series (aggregation). Table 2 summarizes the
775 anticipated effects on permutation entropy of a suite of commonly used pre-processing
776 methods. In many cases, whether a method increases or decreases permutation entropy will
777 depend on the specific attributes of the time series (e.g., its embedding dimension,
778 autocorrelation, covariance structure, etc.) and the permutation order (m) at which its
779 permutation entropy is approximated. This is illustrated by specific examples in figure 3
780 which contrasts the permutation entropies (using $m = 3$) of three hypothetical time series

781 before (top row) and after (bottom row) the application of (a-b) linear detrending, (c-d) log-
782 transformation, (e-f) interpolation of a missing or removed data point with a cubic smoothing
783 spline. As these examples illustrate, with the exception of affine transformations, every pre-
784 processing method discussed has the ability to alter our estimation of how much predictive
785 information is contained in a time series. As such, performing pre-processing of a time series
786 before permutation entropy is determined is not recommended. If the question to be
787 addressed depends on such pre-processing, then care must be taken to understand how
788 preprocessing is affecting the information estimate.
789

790 **Tables**

791 **Table 1:** Model table presenting fixed effects of the mixed model analysis relating
 792 forecasting error to permutation entropy (PE), and additional time series covariates.
 793 Parameter estimates (*B*), 95% confidence intervals (CI) and p-values are provided.
 794 Forecasting error increases with weighted permutation entropy across 461 ecological time
 795 series.

	Forecasting error (nRMSE)		
	<i>B</i>	<i>CI</i>	<i>p</i>
Fixed Parts			
(Intercept)	0.0893	0.0106 – 0.1681	.027
PE	0.4796	0.3944 – 0.5648	<.001
Type (lab)	-0.0751	-0.2988 – 0.1486	.511
Sample size (N)	-0.0017	-0.0021 – -0.0013	<.001
Zero prop.	0.4062	0.0719 – 0.7405	.018
Ties prop.	-0.3344	-0.7698 – 0.1009	.133
Embedding dimension (E)	0.0088	0.0051 – 0.0124	<.001
Nonlinearity (theta)	0.0113	0.0072 – 0.0154	<.001
PE:type (lab)	0.1006	-0.1714 – 0.3726	.469

796

797 **Table 2.** Summary of the anticipated effects on permutation entropy of a suite of commonly used pre-processing methods.
 798

Data processing method	Examples	Effect on		Remark
		Permutation entropy (PE)	Weighted permutation entropy (WPE)	
Detrending	Linear, nonlinear (e.g., GAM), differencing	Increase or decrease	Increase or decrease	Effect will depend on attributes of the time series for any chosen permutation order > 2.
Transformation	$(x - \bar{x})/\sigma$, $\log(x)$, $\sqrt[4]{x}$, Fisher, etc.	None	Increase, decrease, or none	Normalization or rescaling will have no effect as long as the transformation is linear. Nonlinear transformations that compress large values (e.g., $\log(x)$) will increase WPE. Nonlinear transformations that amplify large values (e.g., Fisher) will decrease WPE.
Gap or	Missing data	Increase or	Increase or	Zeros should be retained if they represent true species absences

sequence removal	(NAs), below detection level (zeros), species absences (zeros), constant values (poor precision)	decrease	decrease	(decreasing PE and WPE). Otherwise zeros and constant values can be removed (increasing or decreasing PE and WPE, <i>see main text</i>) or replaced by uncorrelated noise (increasing PE and WPE). The effect of concatenation will depend on attributes of the time series and gap size. Better to not count words that bridge gaps.
Interpolation	To infer gaps or to make time series equidistant	Increase or decrease	Increase or decrease	More likely to decrease than increase. Increases may occur for some nonlinear methods depending on attributes of the time series and the chosen permutation length. Better to ignore time-step uncertainty, assume equidistance, and not count words that bridge gaps.
Smoothing	Time- averaging, time- summation	Decrease	Decrease	Like linear interpolation decreases PE and WPE by increasing the count of only-ascending or only-descending permutations.

Downsampling	Regular subsetting to increase time- step size	Increase or decrease	Increase or decrease	Effect will depend on attributes of the time series (particularly its intrinsic embedding dimension) and the chosen permutation length.
Time series aggregation	Combining species to functional group	Increase or decrease	Increase or decrease	Effect will depend on attributes of the time series being aggregated (e.g., their relative magnitudes, covariance, etc.).

799 **Figure legends**

800 **Figure 1.**

801 A) The total information content of an observation of a system at a given state in time, S_t , is
802 depicted by filled circles with past states (S_{t-1} and S_{t-2}) represented by shades of grey. i) lack
803 of overlap between past and present states illustrating a case where no information is
804 transmitted from past states (i.e. a purely stochastic system), with low redundancy and high
805 Shannon entropy rate, ii) intermediate overlap indicating a case when some information is
806 transferred from past to present (i.e. a deterministic system strongly driven by stochastic
807 forcing), with intermediate redundancy and Shannon entropy rate, iii) large overlap indicating
808 a case when the current state is mostly determined by the previous state (i.e. a highly
809 deterministic system), with high redundancy and low Shannon entropy rate. Note that both
810 the redundancy and Shannon entropy rate of a system are intrinsic properties of the system
811 and will only change if the system itself changes.

812 B) The total information of an observation (black circle) is composed of new information and
813 redundant information; redundant information is composed of active and lost information. A
814 system's redundancy determines its intrinsic predictability. Information may be lost due to
815 observation error and data processing (*lost information*). This reduces the redundant
816 information that can be used for forecasting (*active information*). Lost information is not an
817 intrinsic property of the system but rather represents practical limitations on our ability to
818 make accurate measurements. The rate at which new information is being generated
819 (Shannon entropy rate) may be approximated with permutation entropy. Because permutation
820 entropy quantifies the joint contribution of the Shannon entropy rate and the lost information,
821 efforts that minimize the amount of lost information not only maximize the redundant
822 information that can actively be used for forecasting but also improve the estimation of the
823 intrinsic Shannon entropy rate.

824 C) The realized predictability is the degree to which forecast models can exploit the active
825 information of a time series. Consider, for example, a time-series on the abundance of a
826 species (black line) of which the first 21 days are used to train (parameterize) three
827 forecasting models: a forecast that uses the simple mean of the training data set (red), an
828 Autoregressive integrated moving average (ARIMA) model (green), and an Empirical
829 Dynamical Model (EDM, blue). The forecasting performance of these models is assessed
830 using the remaining time series (after day 22). The inset shows the normalized root mean
831 squared error (nRMSE) as a measure of deviation between predicted and observed values (i.e.
832 forecast error) for each of the three forecasting models. ARIMA and EDM exploit the
833 available structure in the data better than the mean forecast, as illustrated by the coloured
834 wedges filling different amounts of the area of active information.

835 D) In the relationship between PE and FE a system can be moved toward the ideal grey
836 boundary with forecast models that make better use of active information or by reducing
837 information loss, not necessarily in that order. The two panels depict how to reach the
838 greatest achievable forecasting skill in two different systems that have the same initial
839 permutation entropy but differ in their relative amounts of new and redundant information
840 (i.e. they differ in their intrinsic predictability). As these intrinsic properties of the system
841 cannot be changed, improvements to forecast skill rely on fully exploiting the active
842 information available (e.g., improved forecasting model) and minimizing information loss
843 (e.g., improved sampling) to better approximate the true Shannon entropy rate, which
844 establishes the lower boundary (grey area).

845

846 **Figure 2.** We illustrate how to estimate permutation entropy from an empirical time series
847 (A) assuming $m = 3$ and $\tau = 1$. A permutation order $m = 3$ allows for a set of 6 (i.e. $3!$)
848 permutations, shown in panel B. The occurrence of each permutation π is then counted and

849 divided by the total number of permutations as an estimate of their proportional frequency
850 (panel C). For example, permutations 2-3-1 (shown in red) and 3-2-1 are each only found
851 once in the time series, whereas 1-2-3 and 3-1-2 are found twice, leading to frequencies of
852 0.17, 0.17, 0.33 and 0.33, respectively. The permutation entropy is then calculated as the
853 Shannon entropy of proportional frequencies. For the given time series this is 1.92, which is
854 normalized by $\log_2(3!)$ yielding a permutation entropy of 0.74.

855

856 **Figure 3.** Anticipated effects of a suite of commonly used pre-processing methods
857 on (non-weighted) permutation entropy (PE) using three hypothetical time series before (top
858 row) and after (bottom row) the application of (a-b) linear detrending, (c-d) log-
859 transformation, and (e-f) interpolation of a missing or removed data point with a cubic
860 smoothing spline.

861

862 **Figure 4.** Simulations of the deterministic logistic map with no added process or observation
863 noise. A) The last 30 time steps of three times series are plotted to demonstrate different
864 behaviors, including 2-point limit cycles ($r \approx 3.41$; dark blue), chaotic behavior ($r \approx 3.73$;
865 green), and 3-point limit cycles within the chaotic realm ($r \approx 3.84$; gold). B) A bifurcation
866 diagram of the logistic map attractor for growth rates between $r = 3.4$ and 3.9 . C) Weighted
867 permutation entropy (WPE) of the logistic map time series as the growth rate, r , changes for
868 permutation order, m , of 3 (light grey), 4 (dark grey) and 5 (black), and time delay, τ of 1. D)
869 forecast error quantified by the normalized root mean squared error (nRMSE) of an EDM
870 forecast ($E = 2$, $\tau = 1$) of the last 200 time steps of each simulation plotted against WPE
871 ($m=5$, $\tau=1$). The color coding corresponds to the growth rates in 'B'.

872

873 **Figure 5.** The relationship between weighted permutation error (WPE; $m=5$, $\tau=1$) and
874 forecasting error (measured as nRMSE) at three levels of A) process noise and B)
875 observational noise. As the y-axis range and scale changes between subplots, the ‘no noise’
876 case is plotted in grey as a visual reference. The color coding corresponds to the growth rates
877 in figure 4B. Systems with higher process noise exhibit both higher WPE and higher
878 forecasting error. WPE is robust to observational noise when dynamics are chaotic, however
879 limit cycles cause elevated estimates of WPE dependent on the choice of m and τ .

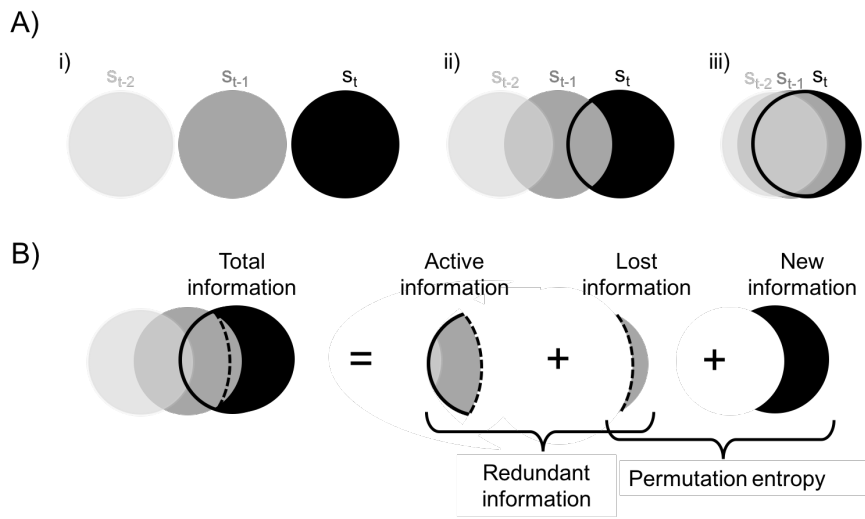
880

881 **Figure 6.** Relationship between weighted permutation entropy and forecast error (nRMSE,
882 note square root scale of y axis) across 461 time series (middle panel) and specific exemplary
883 time series (observations in black, forecasts in red, a-f). Forecast error increases with
884 complexity of the time series as indicated by the higher permutation entropy value. The slope
885 of the relationship was the same for time series from field and laboratory systems. The upper
886 panels (a-c) show time series with forecast error lower than (a) or as expected (b-c) given
887 their level of complexity, whereas the lower panels (d-f) illustrate time series which have
888 higher than expected forecast error.

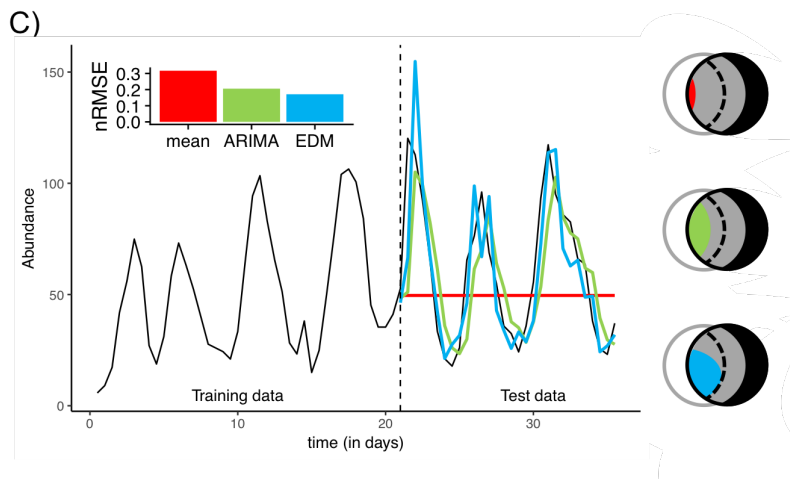
889

890 **Figures**

891

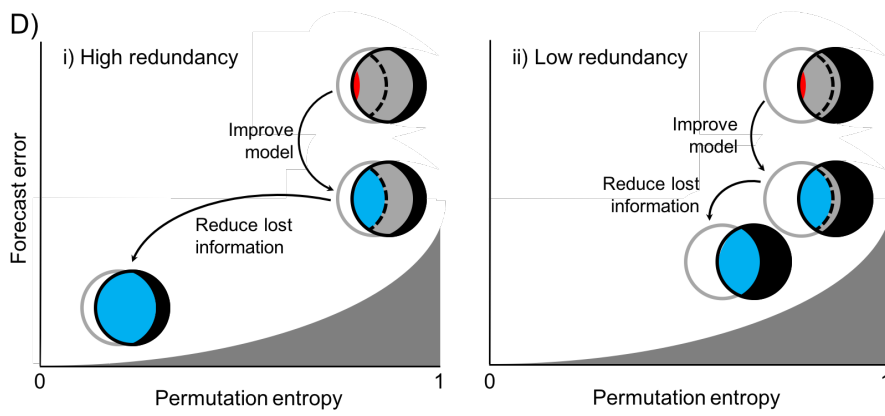


892



893

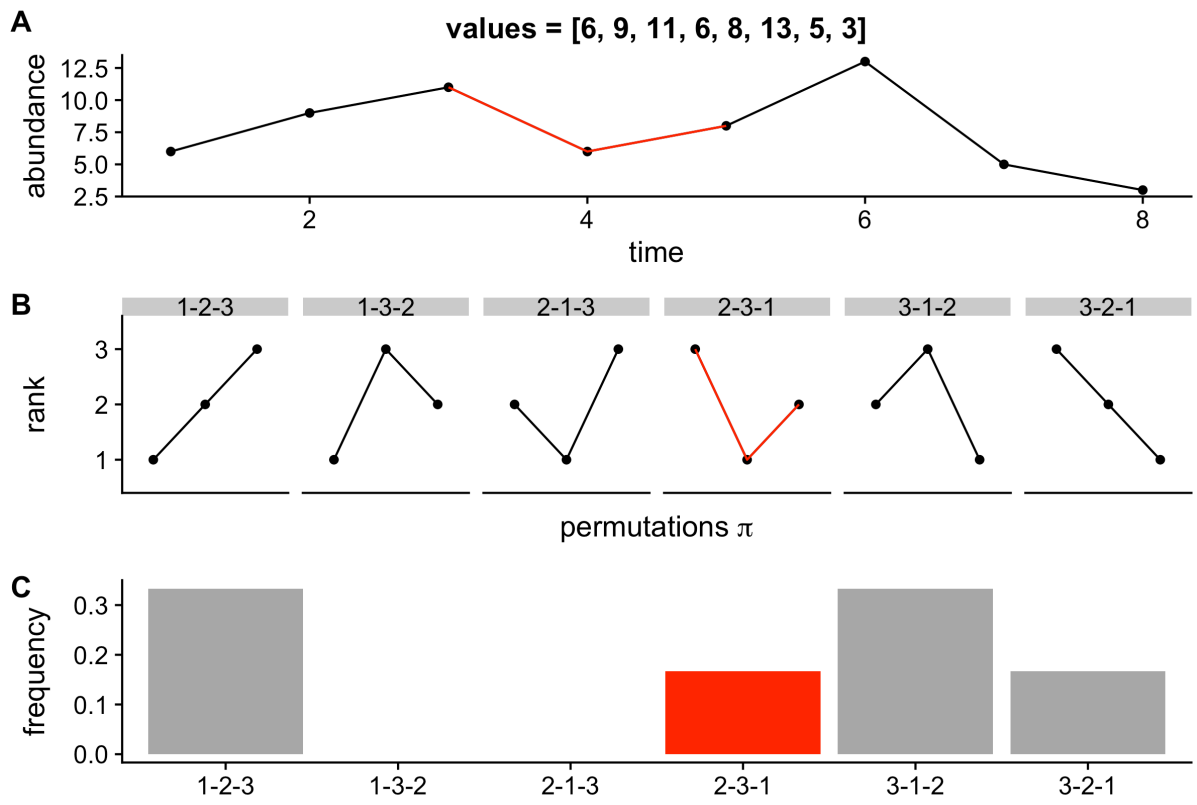
894



895

896 **Figure 1**

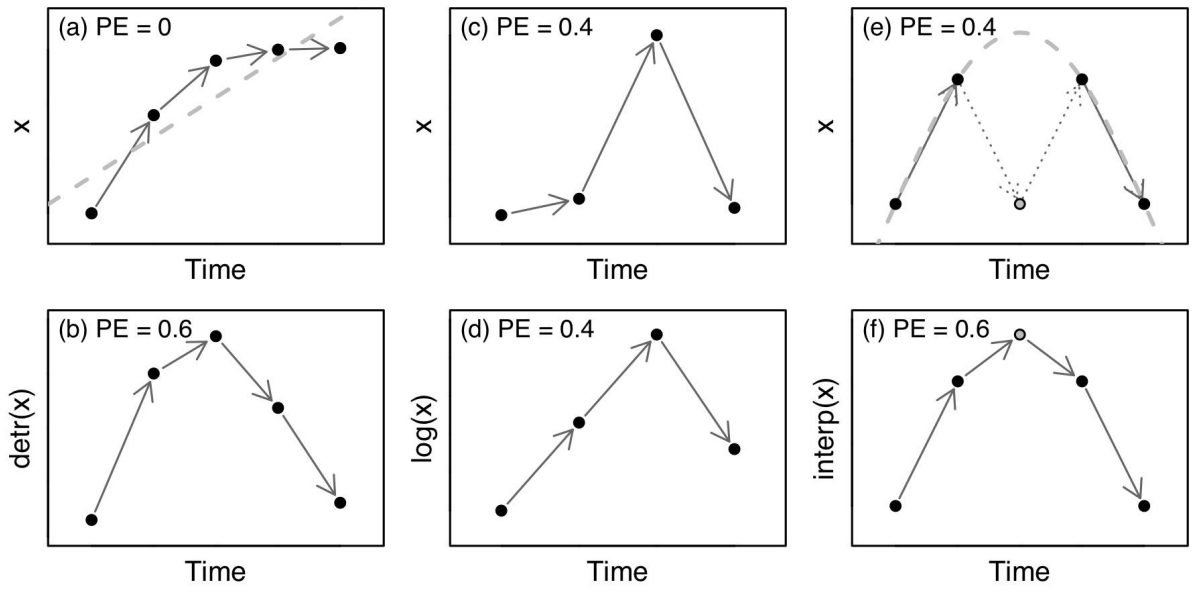
897

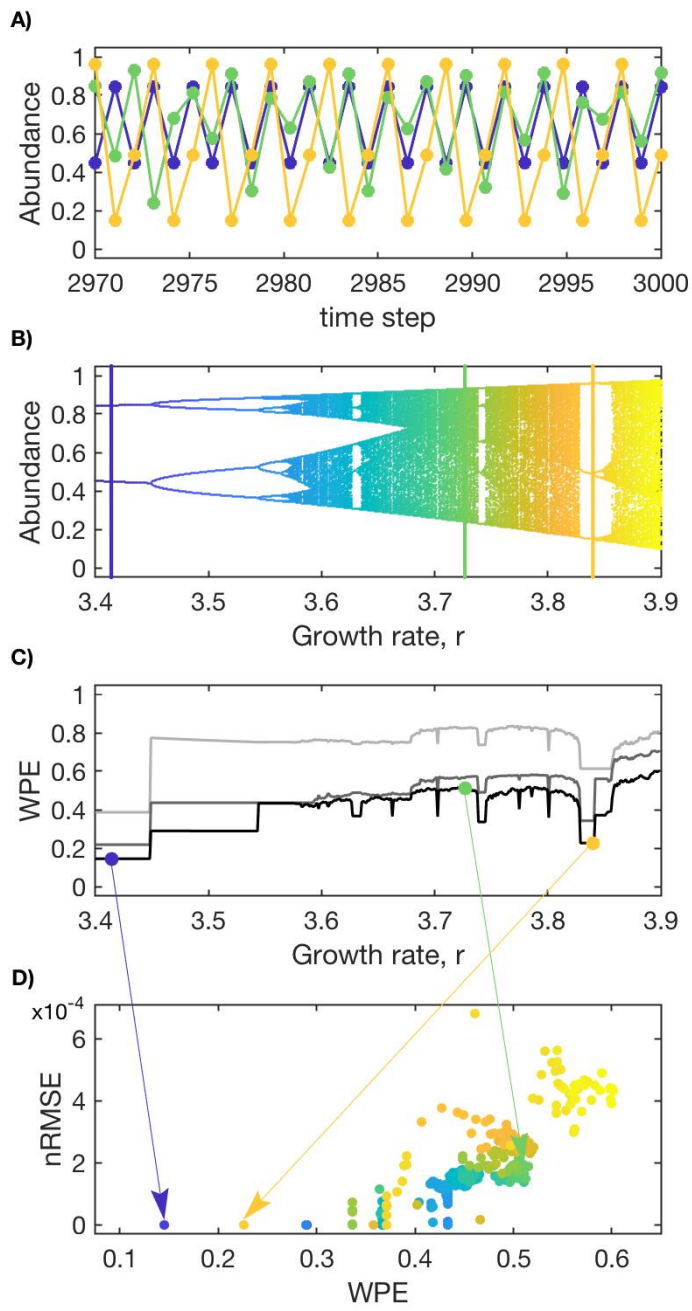


898

$$\text{Permutation entropy} = - \sum_{\pi \in \mathcal{S}_m} p(\pi) \log_2(p(\pi))$$

899 **Figure 2**

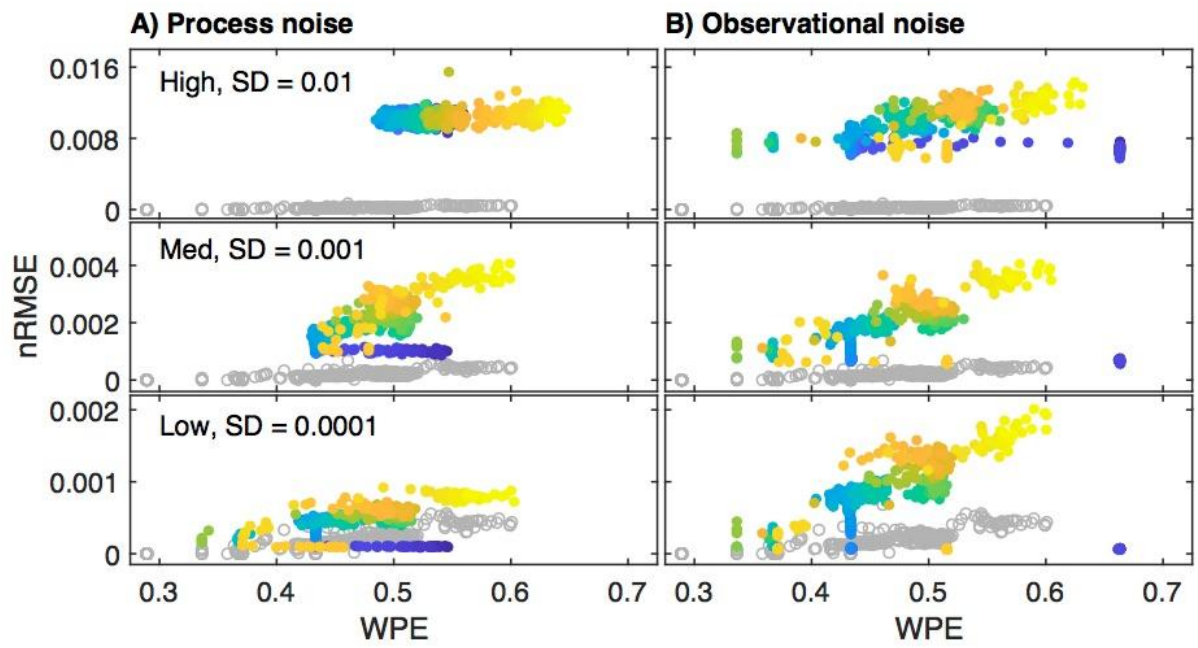




902

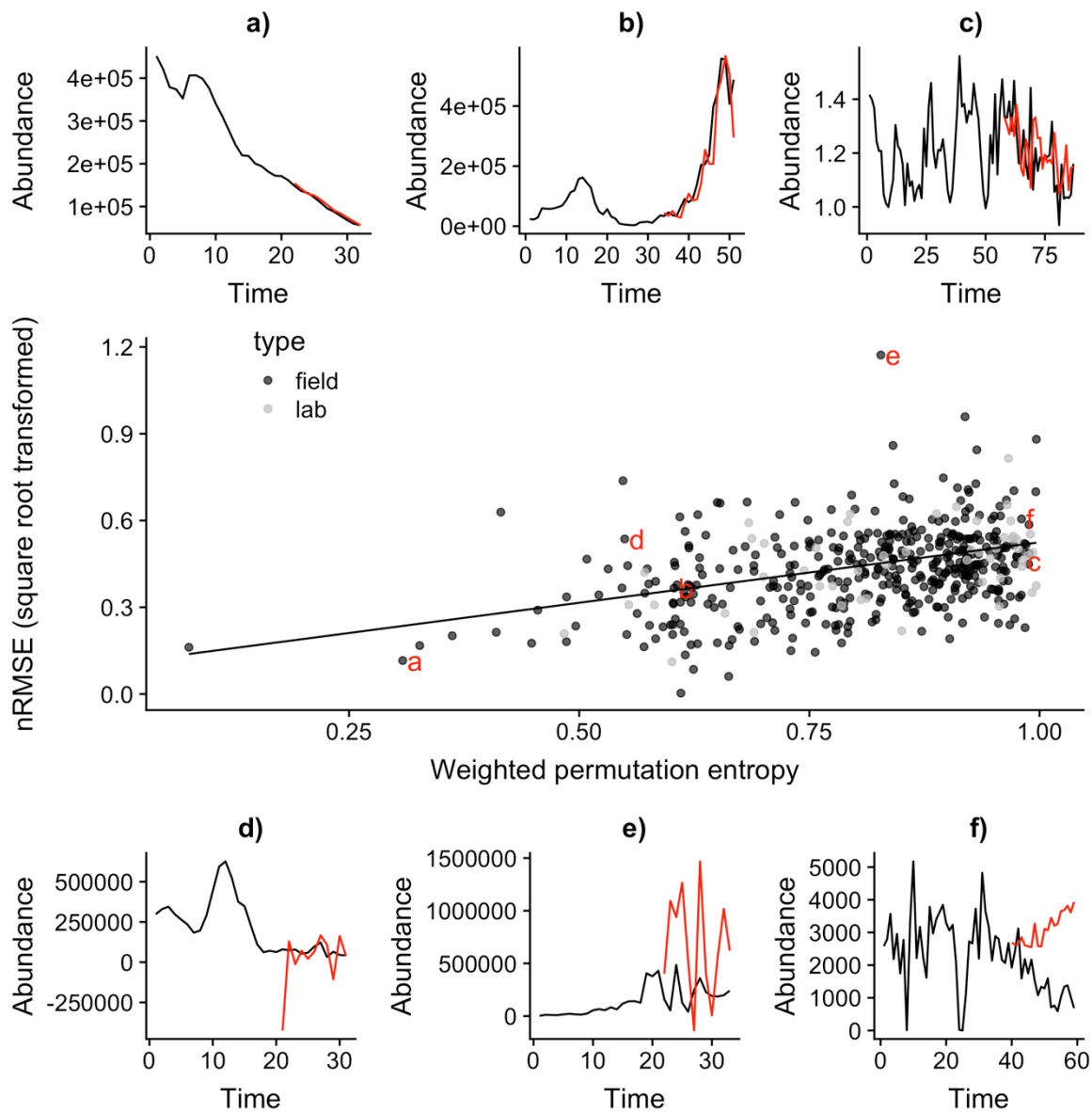
903 **Figure 4**

904



905

906 **Figure 5**



907

908 **Figure 6**